Enhancement of luminescence by pulse laser annealing of ionimplanted europium in sapphire and silica

N. Can, P. D. Townsend, D. E. Hole, H. V. Snelling, J. M. Ballesteros et al.

Related Articles

A phase-cut method for multi-species kinetics: Sample application to nanoscale defect cluster evolution in alpha iron following helium ion implantation
Appl. Phys. Lett. 102, 011904 (2013)

Influence of isothermal hot pressing-doping treatment on the electrical and mechanical properties of bulk Bi-Sr-Ca-Cu-O
AIP Advances 2, 042183 (2012)

Site preference of cation vacancies in Mn-doped Ga2O3 with defective spinel structure
Appl. Phys. Lett. 101, 241906 (2012)

Low cost ion implantation technique
Appl. Phys. Lett. 101, 224104 (2012)

Forward and back energy transfer between Cu2+ and Yb3+ in Ca1−xCuSi4O10:Ybx crystals
J. Appl. Phys. 112, 093521 (2012)

Additional information on J. Appl. Phys.

Journal Homepage: http://jap.aip.org/

Journal Information: http://jap.aip.org/about/about_the_journal

Top downloads: http://jap.aip.org/features/most_downloaded

Information for Authors: http://jap.aip.org/authors

Enhancement of luminescence by pulse laser annealing of ion-implanted europium in sapphire and silica

N. Can, P. D. Townsend,[a] and D. E. Hole
Department of Physics, University of Sussex, Brighton BN1 9QH, United Kingdom

H. V. Snelling
Department of Applied Physics, University of Hull, Hull HU6 7RX, United Kingdom

J. M. Ballesteros and C. N. Afonso
Instituto de Optica, Consejo Superior de Investigaciones Científicas, Serrano 121, Madrid 28006, Spain

Sapphire (Al_2O_3) and silica samples have been implanted with 400 keV europium ions at fluences between 5×10^{14} and 1×10^{16} ions cm^{-2}. As-implanted, samples show luminescence at 622 nm, and although the intensity may be increased by furnace anneals up to 1000 °C, higher temperatures, to 1200 °C, result in less emission, as the impurity ions form precipitate clusters. This problem can be avoided by the use of pulsed laser anneals which dissociate the clusters and quench in atomically dispersed ions. The luminescence intensity has been increased by factors of 95 and 85 for sapphire and silica, respectively, relative to the initial implanted signal. On comparing with furnace anneals at 1200 °C, the pulsed laser annealing is more effective, by factors of up to 45 times. Data for pulsed excimer and CO_2 lasers are compared. Both types of laser appear to remove the ion-implanted radiation damage, but in the case of silica, higher luminescence performance was obtained with the excimer anneals. There was no evidence for diffusion of the implanted europium, as assessed by Rutherford backscattering spectrometry. © 1995 American Institute of Physics.

I. INTRODUCTION

Ion beam implantation is a convenient technology for modifying the surface properties of insulators, and the changes include alterations in the surface reflectivity and the fabrication of optical waveguides, laser and second-harmonic waveguides, upconversion, and nonlinear surface layers. Many of the guide structures have been made by helium or hydrogen ion implantation which define the refractive indices of the guides by generating a low index boundary layer. Hence, the implanted ions are effectively inert with respect to the other changes.[1,2] Alternatively, one may implant active species, such as rare earth ions, which could form the basis of surface lasing regions. Previous attempts to form lasers by implanting Er ions have been unsuccessful, and it is clear that the problem is not one of radiation damage, as this will be annealed at the highest temperatures, but instead is linked to the short range diffusion of the Er which allows the formation of new structural phases or precipitates. It is also probable that at the high temperatures the mobility of the rare-earth ions will show an equilibrium between formation and dissolution of the clusters. Hence the problem is that the thermodynamics of the slowly cooled furnace heated material favor the retention of the clusters, whereas, at least in principle, rapid quenching might retain atomically dispersed Er ions. The challenge is therefore, both to remove the radiation damage, and also to dissociate the rare earth clusters, which form as a result of the highest temperature anneals. For this purpose, pulsed laser annealing was applied to the samples, either directly to the as-implanted samples, or after furnace annealing. If the clusters primarily form during the

cooling cycle, then very rapid cooling might inhibit their growth. The ion-implanted surface is the only region heated by energy from short laser pulses at wavelengths which are strongly absorbed, as is the case for ArF and CO_2 wavelengths, and thus this surface layer can rapidly dissipate the heat into the bulk material. The situation is ideal for defect annealing and fast quenching.

Laser annealing has been used with ion-implanted semiconductors and metals,[3–6] but the literature for insulator targets is very limited.[7–9] Studies of ion-implanted Ag colloids in glass showed dissociation of the colloids using pulsed excimer laser annealing[7] and for Eu rare-earth colloids a similar dissociation of the clusters was indicated.[7,8] In this article, a more extensive study is reported, following doping of Al_2O_3 and silica by 400 keV europium ion implantation, in which the luminescence intensity is greatly enhanced by laser pulse heating at either ArF excimer or CO_2 wavelengths.

II. REVIEW OF Er-IMPLANT DATA

The literature of doping insulators with rare-earth ion beams is not new,[9–11] but is limited in extent. There is a particular interest in forming waveguide lasers for use in optical communications and consequently several research groups have made detailed studies of erbium implantation into a range of target materials to make Er lasers operating at 1.54 μm. Nevertheless, despite numerous progress reports on Er implants into many targets, and a variety of furnace annealing treatments, to date this has not been successful in terms of lasing. The basic problem is that the implantation of the relatively heavy ions produces considerable damage, or amorphization of the target lattice, with a consequent reduction in excited state lifetimes and low luminescence efficiency. Furnace annealing, whether conventional[12–14] or

[a]Electronic mail: p.d.townsend@sussex.ac.uk

rapid,[15] is effective in removing much of the radiation damage and hence increasing both lifetime and luminescence efficiency, but for sapphire or silica the heating cycles must reach 1200 °C to totally eliminate the damage. Unfortunately, at such temperatures the erbium becomes mobile and may precipitate into clusters or complexes. These are nonradiative and the overall light intensity is greatly reduced. The relative signal levels for Er in sapphire and silica range, respectively, from 1 to 40, and from 1 to 4 for the initial intensity compared with the results of annealing at 1000 °C. The data for silica show that a further annealing to 1200 °C in fact reduces the enhanced Er signal by a factor of 20 (i.e., to less than the as-implanted value).

In a recent example with ion-implanted Er in $LiNbO_3$ rapid thermal treatment (RTA) and conventional furnace annealing were compared.[15] They showed that tube furnace annealing gave rise to a significant widening of the Er depth profile, as expected from conventional diffusion. By contrast, RTA suppressed the Er diffusion beyond the implant range, although there was radiation enhanced diffusion toward the surface (but not into the interior). Comparable data have not been reported for the hosts of sapphire and silica.

III. LUMINESCENCE FROM RARE-EARTH DOPANTS

Although the ultimate aim is to use Er ions, for experimental convenience the present ion choice was Eu. This is because Eu emits in the red region of the spectrum near 622 nm and the luminescence analysis was made with a cathodoluminescence (CL) system which was designed for photomultiplier detection. The system was not easily extended into the infrared region for Er signals at 1.54 μm. However, the change in ion species is not thought to be of major importance in terms of the annealing response, since the behavior of rare-earth ions of comparable ionic radius is unlikely to vary greatly. The ionic radius of Eu is some 7% more than that of Er. Al_2O_3 is an especially interesting material for rare-earth doping because of the similarity in valency and lattice constants between Al_2O_3 and Eu_2O_3.[16] These parameters should allow the incorporation of high concentrations of Eu in the Al_2O_3 crystal structure without excessive lattice strain. Nevertheless, the luminescence intensity will be limited by concentration quenching. The implant dopant range spanned a factor of 20 from 5×10^{14} to 1×10^{16} ions per cm^{-2}. In the present experiment ion implantation presents some minor problems, in that the implanted profile is a Gaussian shape. Therefore there is a nonuniform impurity concentration with depth and consequently, if the lifetime or luminescence efficiency is concentration dependent, the measurements will include a convolution of these effects. Nevertheless, by using a range of dopant levels one might assess the significance of such distortions. In future studies it may be helpful to vary the implant ion energy and dose, thereby producing a flatter concentration of impurities with depth in the host material. At our lowest implant dose, of 5×10^{14} ions cm^{-2}, the peak rare-earth concentration is below 0.1%, which may well mark the onset of concentration quenching, as noted not only for Er-implanted data,[14] but also in luminescence dosimetry measurements involving rare-earth ions in hosts as diverse as CaF_2, $CaSO_4$, and MgB_4O_7.[17–19] Con-

sequently, the luminescence intensity will not be a linear function of dose as, at the higher implant concentrations, close neighbor interactions will reduce the emission intensity. Such effects may be partially offset by reductions in excited state lifetime, which will raise the luminescence efficiency.

In practice the earlier Er data did not show great differences in annealing behavior between sapphire and silica, although the two systems result in different Er excited state lifetimes. The preliminary results of Eu implantation confirmed this general pattern of furnace annealing with several targets including Al_2O_3, silica, and float glass. The Er results showed that, while there were some differences between conventional furnace anneals and rapid thermal anneals, in terms of the long range diffusion of the implanted Er, the luminescence efficiency was not significantly improved by rapid heating on the time scale of minutes. By contrast, pulsed laser annealing is orders of magnitude more rapid with the power being delivered on the time scale of 12 ns for the excimer and 90 ns for the CO_2 laser. In order to raise the temperature of the implanted layer to at least 1200 °C, considerably more power is required from the CO_2 laser. This is because the penetration of the light is probably on the scale of the wavelength, assuming large absorption coefficients ($>10^3$ cm^{-1}), either from restrahl or defect absorption. Only a small percentage of the CO_2 power is absorbed within the depth scale of the implanted Eu (i.e., <200 nm). The subsequent quenching of the laser heated region will be slower for the CO_2 pulses, compared with the excimer treatment, as they involve both more deposited power and a larger volume of material. Overall, these differences might provide a probe to separate pulsed laser annealing of radiation damage from dissolution of clusters and quenching of isolated ions.

IV. EXPERIMENT

The implantations have been performed with Eu^{++} (A =153), at 200 kV (i.e., effectively 400 keV Eu) and a beam current density of between 8 and 16 μA cm^{-2}. The implantation fluences ranged from 5×10^{14} to 1×10^{16} ions cm^{-2}. All implants were performed with the bulk samples kept at 34 °C. Depth analyses were made by Rutherford backscattering spectrometry (RBS) with an analyzing beam of $^4He^+$ with an energy of 1.89 MeV, at a total dose of 50 μC. The backscattering collection angle and detector acceptance angles were $\theta = 150°$ and $\Omega = 0.42$ msr. Using a charged particle beam to analyze insulators can cause the surface to charge up, thereby causing a positive shift of the whole energy spectrum, since the ions enter the surface with a single positive charge, but are fully stripped when they reemerge. The charging problem was overcome by painting colloidal graphite solution onto part of the sample adjacent to the point of measurement. To further reduce the charging problem, a low beam current of around 30 nA was used.

Anneals were made with a standard tube furnace, in an air environment, over a temperature range from 100 to 1200 °C for 1 h intervals. As already mentioned, two types of pulsed laser treatment have been used, these being an ArF excimer or a CO_2 laser. The ArF excimer laser [wavelength = 193 nm and pulse length 12 ns full width at half-maximum

(FWHM)] combined with an homogenizer, irradiated areas of 4×4 mm, within which the homogeneity was better than 3%. The energy density at the sample site was varied in the range 145–390 mJ cm^{-2}. Several pulses (from 100 to 20 000) of the same energy density (within 5%) were accumulated in various areas of the samples at a repetition rate of 1 or 5 Hz. Pulsed CO_2 laser annealing was performed with the same samples at an energy density of 2 J cm^{-2} for silica and sapphire. The CO_2 pulse duration has a FWHM of 90 ns and implanted regions were exposed to from 5 to 5000 shots at a repetition rate of 1 Hz. Throughout the present investigation the CO_2 beam diameter on the samples was maintained at ~2 mm.

For the CL measurements, an electron beam of energy 10 keV has been focused into a spot of 2 mm in diameter. Beam currents of 0.2–0.4 μA were used to excite the samples. It should be emphasized that the broad diameter of the beam significantly reduces any instabilities caused by secondary electron emission. Since changes in ion beam energy and current density may modify the emission spectra and intensity, all spectra shown here were recorded with the same conditions. The electron beam has been chopped at the same modulation frequency, except in the lifetime measurements, and the signal output was measured with a lock-in amplifier. The phase difference between the reference and signal, j, can be measured by the lock-in amplifier, and therefore the excited state lifetime, t, can be obtained from the relationship $\tan j = 2\pi f t$,[20] where f is the chopping frequency.

V. RESULTS

A. Sapphire (Al_2O_3)

CL emission spectra have been recorded between 300 and 800 nm for Al_2O_3: Eu at room temperature with different excitation modulation frequencies. Figure 1 depicts CL spectra measured with sapphire after implantation with 5×10^{15} Eu ions cm^{-2} at 400 keV. The data of Fig. 1(a) are for as-implanted crystals, and Fig. 1(b) shows how this signal is modified after furnace annealing at 1000 °C. Note that although the intensity scales on the graphs are presented as "arbitrary units," they nevertheless are consistent throughout. As can be seen from Figs. 1(a) and 1(b), there is a broadband emission near 340 nm, which is characteristic of the sapphire host lattice. The line feature near 694 nm arises from Cr impurities in the host, and the remaining line spectra are from the implanted Eu. The corresponding electronic transitions involved for these emission lines have been assigned on the basis of the known energy level scheme of Eu^{3+} ions.[21] The strongest red emission line observed in all samples, and at all fluences, is at 622 nm, and is assigned to the Eu transitions from the $^5D_0$ to the $^7F_2$ level. The experimental width of the line is 12 nm FWHM for sapphire. This broadened to 18 nm for silica, consistent with inhomogeneous broadening in the glass. The nature of the broadening mechanisms was reported in detail[22] and other transitions from ^5D_j (j=0,1,2,3) levels to other ^7F_j levels (j=0 to 6) spectrum may be observed, however they could not be separated in the present system. No spectral shifts of the Eu emis-
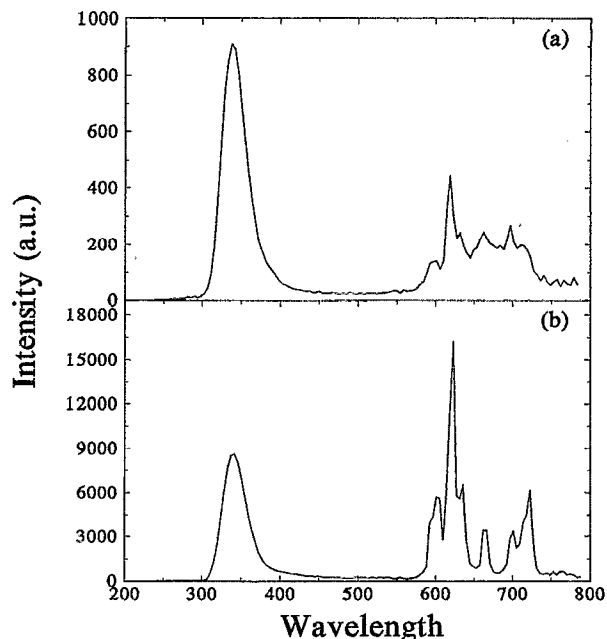

FIG. 1. Examples of room-temperature cathodoluminescence spectra from Eu-implanted sapphire (1×10^{16} Eu cm^{-2}) (a) after ion implantation and (b) after 1000 °C furnace annealing. The lock-in amplifier modulation frequency was 90 Hz. Although in arbitrary units, the scales are consistent.

sion lines have been detected by CL between 77 and 293 K. This is mainly due to the shielding of the electronic levels in the $4f^6$ configuration of Eu ions, by $5s^25p^6$ electrons, from perturbations due to neighboring atoms, i.e., shielding from crystal-field interactions. Spectra from the samples implanted at different fluences have different intensities and similar shapes, but with small variations in relative intensity between the component lines.

Following each furnace annealing from 100 to 1200 °C in air, for an hour at each temperature, the CL intensity for the Eu signal changed as shown in Fig. 2(a). This pattern is very similar to that seen for Er photoluminescence anneal data. There is a gradual increase in CL intensity on annealing up to 600 °C, followed by a further, and more rapid, increase with temperature above 600 °C. For instance, after annealing at 600 °C for the sample implanted with 5×10^{15} Eu ions cm^{-2}, the intensity increases ~fourfold with respect to the original as-implanted signal, and after the 1000 °C anneal the overall intensity has been increased by a factor of 18 times for the Eu signal, but different amounts for the Cr impurity and the intrinsic defect emission. Such variations are a function of the anneal temperature. As with the earlier data of Er-implanted silica, the Eu-implanted sapphire luminescence intensity then falls on annealing to 1200 °C. The supposition in both cases is that the rare-earth ions are no longer randomly dispersed, but instead have clustered into precipitates.

As well as altering the intensity there are changes in the Eu lifetime, and Fig. 2(b) gives lifetime measurements for a sapphire sample implanted at a fluence of 1×10^{16} Eu ions cm^{-2}, and then annealed up to 1200 °C. Figure 3 describes how the 1000 °C anneals influence the CL intensity and lifetime for different doping levels. The lifetime in-
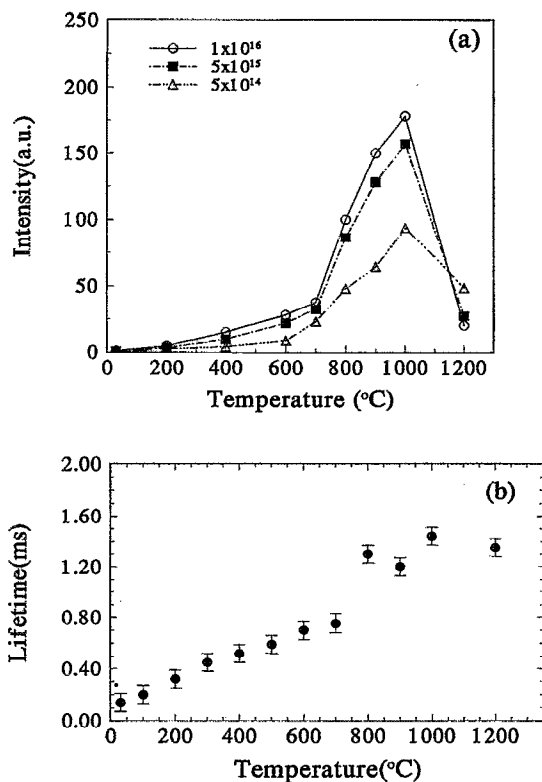
FIG. 2. (a) The 622 nm Eu CL intensity following isochronal furnace annealing, for periods of one hour. The implant levels were 5×10^{14}, 5×10^{15}, and 10^{16} Eu ions cm^{-2}, (b) Lifetime changes with annealing temperature for Al_2O_3 implanted with 1×10^{16} Eu ions cm^{-2}.

creases with increasing anneal temperature and the observed annealing behavior may be examined in two different regions. Comparing the curves of the 622 nm Eu intensity data, with t values below ~700 °C, one notes that both of them exhibit a similar pattern of increase. For different concentrations (C) of implanted Eu, the luminescence signals of optically active Eu, the measured lifetime (t), and CL intensity (L) are given by

$$1/t = 1/t_r + 1/t_{nr},$$

where t_r and t_{nr} are the lifetime associated with radiative and nonradiative decay, and $h = t/t_{nr}$ is the radiative recombina-
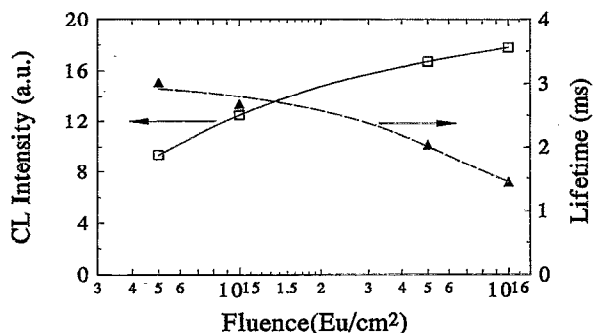

FIG. 3. Cathodoluminescence peak intensity (open square data points, left-hand axis) and lifetime (solid data points, right-hand axis) at 622 nm as a function of Eu fluence in sapphire after annealing at 1000 °C for 1 h.
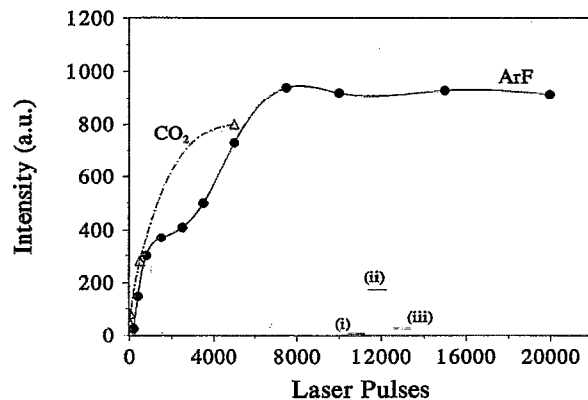

FIG. 4. The Eu 622 nm line intensity in sapphire after either pulsed CO_2 laser treatments (triangles), or after using an excimer laser, with samples implanted with 1×10^{16} ions cm^{-2}. For comparison purposes the markers (i), (ii), and (iii) indicate the CL intensities for "as-implanted" and furnace annealed at 1000 and 1200 °C.

tion efficiency, and L is a function of h and C. In the first approximation, we can assume that $1/t_r$ is constant because we have observed that the CL emission spectra do not change significantly depending on the fluence and annealing temperature. Hence changes in lifetime are mainly due to changes in t_{nr}. According to the equation above, a high nonradiative decay rate ($1/t_{nr}$) gives rise to a low lifetime (t), thereby low CL intensity. Annealing of implantation-induced defects in the sapphire decreases the number of nonradiative paths, and so the lifetime increases. Furthermore, this result is confirmed with studies that show annealing temperatures from 700 to 1200 °C are essential to anneal implantation damage in Al_2O_3.[23] Thermal annealing at temperatures up to 1000 °C increases the CL intensity of the implanted europium by a factor of 20 for the 1×10^{16} Eu ions cm^{-2} case, but the increase in CL intensity is not associated with a significant increase in lifetime.

Note that this behavior is substantially the same as for the earlier Er-implanted silica and sapphire results.[11–14] By contrast, an example with ion-implanted Er in $LiNbO_3$ showed the lifetime is constant for the whole concentration range.[15] The decreases in the values of the lifetime, shown in Fig. 3 are attributed to an increase in the number of nonradiative decay channels, which may result from implantation-induced defects or concentration quenching.[24] Overall, one infers from the annealed low dose situation that the isolated Eu ions have a lifetime in sapphire in excess of 3 ms.

Figure 4 summarizes the results obtained so far for both pulsed CO_2 and the ArF excimer pulsed laser annealing of the Eu-implanted sapphire. The data for the CO_2 pulse annealing can be fitted to a saturating exponential form, as drawn in Fig. 4. Such a dependence on the number of laser pulses is consistent with random annealing events which take place in small volumes, which eventually overlap. It therefore appears that with the present CO_2 laser beam conditions, a maximum luminescence enhancement has been reached. (Note that since only a single CO_2 energy density was used in this experiment there is no guarantee that the optimum luminescence level has been achieved, and a study of the
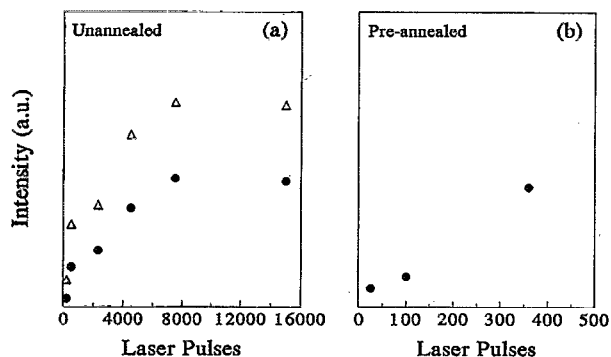
Can et al.

FIG. 5. ArF pulsed excimer annealed sapphire data for (a) laser treatment directly after implantation for implant doses of 5×10^{14} (solid circles) and 5×10^{15} Eu ions cm^{-2} (open triangles); (b) shows data for a sample implanted to a dose of 1×10^{16} Eu ions cm^{-2} but annealed to 1200 °C prior to laser pulse treatment.
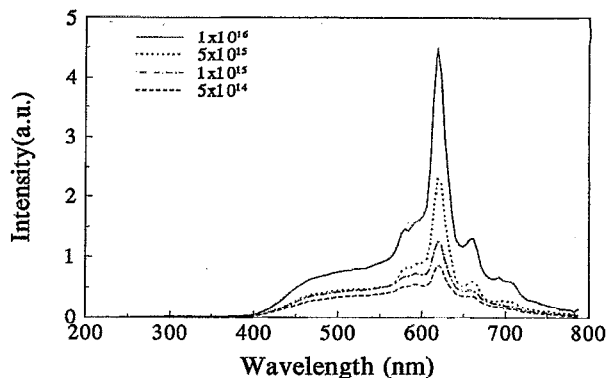

FIG. 6. Cathodoluminescence spectra for Eu-implanted silica at fluences ranging from 5×10^{14} to 1×10^{16} Eu ions cm^{-2}. The lock-in amplifier modulation frequency was 90 Hz.

effects of changing pulse power, or substrate temperature, etc., is required.)

The data using the ArF excimer annealing, are also shown in Fig. 4, for the highest dopant level of 1×10^{16} ions cm^{-2}. This excimer experiment followed from the as-implanted condition and there is not a smooth response with the number of pulses, but instead there is an initial rise, followed by a second increase beyond ~4000 pulses to a saturation after ~7500 pulses. Since annealing may remove radiation damage at a different rate from the dissolution of precipitates, a first interpretation may be that removal of the lattice damage is defined by the first annealing stage. Finally to emphasize the value of the pulsed laser annealing, Fig. 4 includes an indication of the as-implanted intensity level (i) and the level reached following furnace annealing at 1000 °C (ii), and 1200 °C (iii).

Figure 5(a) indicates the dependence of the luminescence for excimer pulse annealing using smaller implant concentrations and Fig. 5(b) emphasizes that the excimer pulses are effectively independent of any furnace anneal treatment as the signal can be enhanced by the laser pulses, even for furnace annealed material. One might claim that the net result of the furnace anneals could be duplicated by ~100 excimer laser pulses (i.e., a processing time of a microsecond rather than hours). The signals from the Cr impurities and from the intrinsic UV luminescence are also changed by the laser anneals, but to a lesser extent than for Eu ions. The Cr line intensity increased by a factor of 60 relative to that recorded initially in the as-implanted sample, and the broad 340 nm peak intensity rose by a factor of 20.

The excimer annealing also caused some further increases in the lifetime for the 622 nm signal and the values reached 1.53 ms following 360 laser pulses into the 1×10^{16} ions cm^{-2} sample, rising to 1.58 ms after 20 000 pulses. These values compare with the 1.44 ms reached after 1000 °C furnace annealing. The highest value recorded for the implanted Eu is ~3 ms for the lightly doped crystal after 1000 °C annealing. This implies that with optimum processing a number in excess of 3 ms should be achievable if one avoids concentration quenching.

B. Silica

Figure 6 shows room temperature CL spectra of a series of silica samples implanted from 5×10^{14} to 1×10^{16} Eu ions cm^{-2} at 400 keV. The spectra peak at 622 nm, and include additional Eu lines together with a broadband signal extending from 400 to 800 nm. Relative to the Al_2O_3 samples, the silica samples initially exhibit a stronger CL intensity after implantation for all fluences. For the furnace annealing measurements results, comparable to those of sapphire were obtained with Eu-implanted silica samples. The data are consistent with those seen for the earlier Er implant. After the implantation, all silica samples have been isochronally annealed in the temperature range from 100 to 1200 °C in air for 1 h. The overall shape of the spectra were similar for the different fluences, ranging from 5×10^{14} to 1×10^{16} Eu ions cm^{-2}, as shown in Fig. 6. However the broadbands, underlying the line features, were removed during annealing. The pattern of annealing curves for the 622 nm signal are similar for each dose, Fig. 7(a). Lifetime changes are given by Fig. 7(b) for the highest dopant level. These lifetime data follow the familiar pattern of annealing up to a plateau value. Figure 8 combines data on the the concentration dependence of signals recorded after the 1000 °C annealing. As can be seen from Fig. 8, a reduction in the lifetime from 9 to 5.5 ms is observed with increasing Eu-implantation fluences but presumably even longer lifetimes should exist for more dilute systems. These are relatively long lifetimes compared with those of Eu in sapphire. Note however that the same implantation dose represents a higher local dopant concentration in sapphire, because the ion range is less than for silica. Also, in hindsight one realizes that for the long lifetime states of the Eu in silica, the use of a 90 Hz lock-in amplifier detection may in fact slightly reduce the amplitude of the annealed sample signal.

Figure 9 shows the results of pulsed CO_2 annealing on Eu in silica, for a sample implanted to a dose level of 5×10^{15} ions cm^{-2}. Also presented in Fig. 9 are data for annealing, using excimer laser pulses, into a sample implanted, in this case, with a higher Eu dose of 1×10^{16} ions cm^{-2}. Two factors are involved that result in improvements in the luminescence efficiency. One is the removal of the radiation damage, which would give nonradiative decay, and the other is the

J. Appl. Phys., Vol. 78, No. 11, 1 December 1995

Can *et al.*   6741

FIG. 9. The 622 nm intensity following pulsed CO_2 laser annealing of an as-implanted $(5 \times 10^{15}$ ions $cm^{-2})$ silica sample (squares), compared with data for samples illuminated with a pulsed excimer laser at different energy densities. Note this latter sample contained a higher Eu implant dose $(1 \times 10^{16}$ Eu ions $cm^{-2})$.
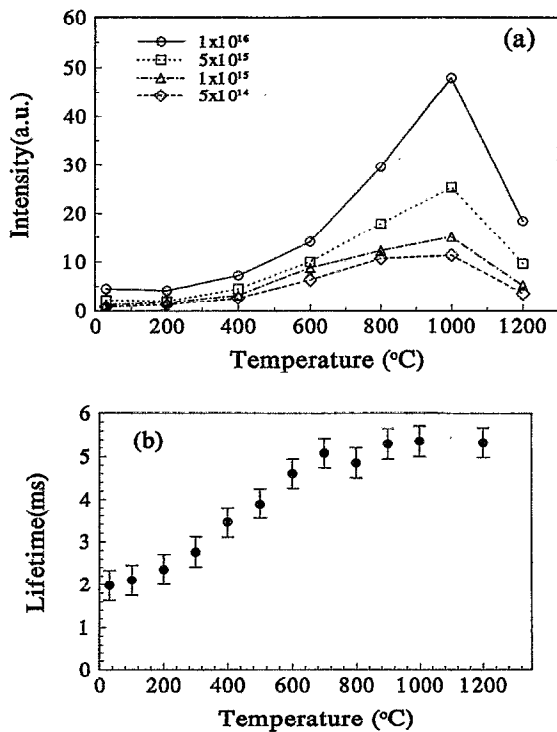
FIG. 7. (a) The 622 nm Eu CL intensity from silica after furnace annealing for different ion doses; (b) The Eu lifetime vs anneal temperature for a silica sample implanted with 1×10^{16} Eu ions cm^{-2}.

distribution of the Eu into isolated noninteracting sites. Overall, the increase in CL intensity follows a saturating exponential dependence with pulsing of the CO_2 laser, as did the sapphire. By contrast, the pulsed excimer data has a shoulder region developing after about 1000 pulses. The development of the higher plateau level has been followed for the lower excimer pulse power up to 10 000 pulses, and an equilibrium is reached by ~5000. The form of the curves is apparently insensitive to excimer pulse power in the range used, as the data are very similar for both the 145 and 390 mJ cm^{-2} sets of pulses. This is perhaps surprising, but one must recognize that in addition to defect annealing the quenching of dispersed precipitate phases will be dependent on the speed of cooling as the material moves down to the temperature range
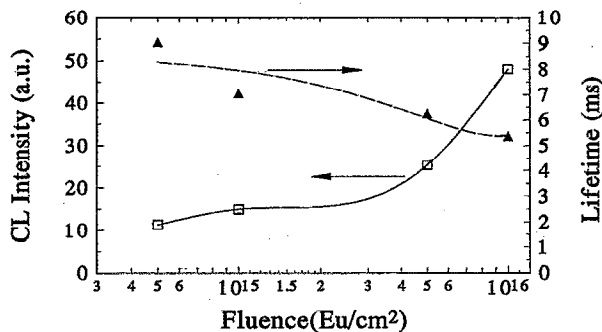

FIG. 8. The CL intensities and lifetimes measured at 622 nm for Eu-implanted silica as a function of Eu fluence. The silica was previously annealed at 1000 °C for 1 h.
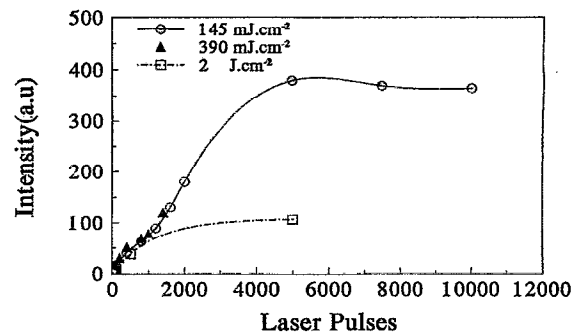
where europium mobility is inhibited. Thus, although the higher powers may generate higher temperatures, the cooling curves may be relatively independent of this upper temperature. The difference in effective heating times between the two power levels is probably only on the nanosecond time scale. Although numerous factors exist, one may argue that, once a critical power level is reached to remove damage and allow restructuring of the glass, then the quenching effects are insensitive to the power. It should be noted that the highest intensities induced by the excimer exceed those from the CO_2 laser by about two times (after adjusting for concentration effects), and these values are some 8 times greater than found after 1000 °C furnace annealing.

VI. GENERAL DISCUSSION

The primary objective of this experiment was to examine if by very rapid pulsed laser annealing it is possible to increase the luminescence intensity and lifetime of rare-earth ion-implanted oxides. The two examples, of a crystalline and a glass target, both emphasize that this is achievable with a very few laser pulses. Since in the case of Er implants in $LiNbO_3$ there was movement of the Er during normal and fast furnace anneals, some measurements were made here to check if the Eu ions had been displaced from their implant distribution. In practice neither the furnace nor the laser anneals induced any movement which could be sensed by Rutherford backscattering spectrometry for Eu in sapphire and silica targets. Tables I(a) and I(b) list the observed and calculated values of the projected ion range, and the range straggling, measured for the Eu ions at different doses. It is seen that these are in good agreement with the computer simulations of such ion range distributions. Similar predictions were obtained from two alternative simulation programs (TRIM[25] and SUSPRE[26]).

The pattern of furnace-induced change on the luminescence intensity is similar for both Eu and Er implants in the sapphire and silica, even though CL was used in the present case and photoluminescence was recorded for the Er examples. Similar behavior is also recorded as a function of implant concentration and Table II summarizes the changes in lifetime and relative intensity for the furnace anneals of

Can *et al.*

TABLE I. RBS data for 400 keV Eu implantation in sapphire and silica. (a) Experimental values; (b) calculated using computer simulations of TRIM (Ref. 25) and SUSPRE (Ref. 26).

(a) Dose (ions cm^{-2})	Projected range (Å) Silica	Projected range (Å) Sapphire	Range straggling (Å) Silica	Range straggling (Å) Sapphire
5×10^{14}	1142	690	290	173
1×10^{15}	1139	691	294	170
5×10^{15}	1141	693	289	172
1×10^{16}	1145	698	285	168

(b)	TRIM Silica	TRIM Sapphire	SUSPRE Silica	SUSPRE Sapphire
Projected range (Å)	1291	753	1156	673
Range straggling (Å)	292	174	192	113

both Er and Eu. The significant improvements brought about by pulsed laser annealing emphasize the scale of improvement which is possible with this new technique. The new data are consistent with other studies of excimer pulse illu-

mination of silica, in which at somewhat higher energy densities of ~400 mJ cm^{-2} defect formation and annealing studies have been made in silica windows[27,28] and in a 650 nm fluorescence.[29]

It is also clear that neither furnace nor laser annealing result in a signal level which increases linearly with dose. For sapphire the intensity of the Eu signal only increases about a factor of 2 for a 20-fold increase in implant dose. The dose dependence of the signal after 1000 °C furnace, or the excimer anneals, is approximately proportional to (concentration)$^{0.2}$, using the three values shown. The silica signal for furnace anneals has a clearly different power dependence, near 0.55, for the four implant doses used. Because of the shorter ion range in sapphire, and more critically, a smaller range straggling, the local Eu concentration in sapphire will be some 50% greater than in silica. The luminescence intensity is the summation of signals within the ion range distribution and the concentration quenching effect changes throughout this volume. Hence, it is not immediately obvious how to associate the measured power law dependence to these features. Nevertheless, one may be tempted to suggest that the 0.55 exponent for silica may

TABLE II. (a) Summary of relative cathodoluminescence intensities of Eu-implanted sapphire and silica after annealing treatment. (b) Photoluminescence data for implanted Er taken from earlier literature.

(a)	Relative intensities with furnace annealing for 1×10^{16} ions cm^{-2} Sapphire	Silica glass
As-implanted	10	4.5
After 1000 °C	178	48
After 1200 °C	20	18.5
After CO$_2$ laser anneal	800	250[a]
After excimer anneal	940	380

Eu lifetime measurements

Eu 622 nm emission

	Sapphire	Silica glass
Maximum lifetime after annealing 1000 °C (ms)	3	9
Reference	Present work at low doses	

(b)	Dose (Er/cm^2)	Energy (MeV)	Annealing temperature (°C)	Lifetime (ms)	Intensity (a.u.)	Intensity (a.u.)
Sapphire	2.3×10^{15}	0.8	As-implanted	1	1	
			1000	7	40	
Reference				5	5	
Silica	5×10^{15}	3.5	As-implanted	6	1	1
			1000	15	4	2
			1200	17	0.2	0.14
Reference				6	6	7
LiNbO$_3$	5×10^{15}	3.5	1060	2.8	1	
	1×10^{16}	3.5	1060	2.8	2	
Reference				8	8	
P-Glass	3.8×10^{16}	2.9	As-implanted	12	1	
			700	12	1.6	
			1000	12	1.2	
Reference				6	6	

[a]Inferred from data with 1×10^{15} Eu ions cm^{-2}.

J. Appl. Phys., Vol. 78, No. 11, 1 December 1995

Can et al.   6743

imply that there is pairing or the Eu ions. This hypothesis would be consistent with rare-earth pairing effects seen in CaF_2, where there is both an ion size and valence mismatch, between the rare-earth ions and the host lattice structure.

Further, as the Eu lifetimes are varying throughout the concentration range, even for the very low Eu concentration, then it is evident that the Eu is influenced by the presence of other Eu ions. Concentration effects are also visible as the result of annealing at 1200 °C. In the case of sapphire the signals fall faster for the highest implant concentration, whereas for the more dispersed material in the silica, the decreases relative to the signals after 1000 °C anneals, remain in sequence. While laser annealing has increased the Eu signal levels, the laser annealed sapphire data follow approximately the same power dependence as for furnace heating, hence the intensity is inherently limited by concentration quenching of independent Eu ions. This suggests that while cluster or precipitation effects may be overcome by the laser annealing, the short lifetimes and nonlinear concentration dependence are still related to a local concentration quenching effect. Hence, the present significant improvements should not be taken as an upper limit in performance. While further improvements may (or may not) be feasible with respect to the cluster problem, by optimizing the laser beam power, wavelength, or bulk sample temperature, it is certain that an overall reduction in the dopant density could increase the signal by an order of magnitude. Consequently, for a laser application, it is essential to disperse the implanted ions over a greater volume of crystal. This is readily achieved by using a range of implant energies and limiting the peak concentration at any depth to the equivalent of say 10^{14} ions cm^{-2}. With such simple adjustments in implantation and annealing techniques, rare-earth ion-implanted lasers may well be feasible.

ACKNOWLEDGMENTS

[1] P. D. Townsend, P. J. Chandler, and L. Zhang, *Optical Effects of Ion Implantation* (Cambridge University Press, Cambridge, 1994).
[2] P. D. Townsend, Nucl. Instrum. Methods B **89**, 270 (1994).
[3] D. Hoonhout and F. W. Saris, Radiat. Eff. **66**, 43 (1982).
[4] M. Von Allmen, *Laser Beam Interactions with Materials* (Springer, Berlin, 1987).
[5] G. Sorensen, Nucl. Instrum. Methods **186**, 189 (1981).
[6] R. A. Wood, P. D. Townsend, N. D. Skelland, D. E. Hole, J. D. Barton, and C. N. Afonso, J. Appl. Phys. **74**, 5754 (1993).
[7] N. Can, P. D. Townsend, D. E. Hole, and C. N. Afonso, Appl. Phys. Lett. **65**, 1871 (1994).
[8] N. Can, B. Yang, D. E. Hole, and P. D. Townsend, Nucl. Instrum Methods B **96**, 397 (1995).
[9] F. J. Bryant, Radiat. Effects **65**, 81 (1982).
[10] A. Krier and F. J. Bryant, J. Phys. Chem. Solids **47**, 719 (1986).
[11] Ch. Buchal, S. P. Withrow, C. W. White, and D. B. Poker, Annu. Rev. Mater. Sci. **24**, 125 (1994).
[12] G. N. van den Hoven, E. Snoeks, A. Polman, J. W. M. van Uffelen, Y. S. Oei, and M. K. Smit, Appl. Phys. Lett. **62**, 3065 (1993).
[13] A. Polman, D. C. Jacobson, D. J. Eaglesham, R. C. Kistler, and J. M. Poate, J. Appl. Phys. **70**, 3778 (1991).
[14] A. Polman, A. Lidgard, D. C. Jacobson, P. C. Becker, R. C. Kistler, G. E. Blonder, and J. M. Poate, Appl. Phys. Lett. **57**, 2859 (1990).
[15] F. Fluester, Ch. Buchal, E. Snoeks, and A. Polman, Appl. Phys. Lett. **65**, 225 (1994).
[16] P. Villars and L. D. Calvert, *Pearson's Handbook of Crystallographic Data for Intermetallic Phases* (American Society for Metals, Metals Park, OH, 1986).
[17] K. S. V. Nambi, V. N. Bapat, and A. K. Ganguly, J. Phys. C **7**, 4403 (1974).
[18] M. Prokic, Rad. Prot. Dosim. **151**, 603 (1978).
[19] S. W. S. McKeever, M. Moscovitch, and P. D. Townsend, *Thermoluminescence Dosimetry Materials: Properties and Uses* (Nuclear Technology Publishing, Ashford, 1995).
[20] M. Demtroder, *Laser Spectroscopy* (Springer, Berlin, 1981).
[21] S. Hufner, *Optical Spectra of Transparent Rare-Earth Compounds* (Academic, New York, 1978).
[22] R. M. Farlane and A. A. Kapplyanskii, *Spectroscopy of Solids Containing Rare Earth Ions* (North-Holland, Amsterdam, 1987).
[23] Y. Chen, M. M. Abraham, and D. F. Pedraza, Nucl. Instrum. Methods, B **59/60**, 1163 (1991).
[24] G. W. Arnold and P. Mazzoldi, in *Ion Beam Modification of Insulators*, edited by P. Mazzoldi and G. W. Arnold (Elsevier, Amsterdam, 1987).
[25] J. P. Biersack and L. G. Haggmark, Nucl. Instrum. Methods **174**, 257 (1980).
[26] R. P. Webb, Surrey University Sputter Profile from Energy Deposition, (SUSPRE) Practical Surface Analysis. Ion and Neutral Spectroscopy, New York, 1992 (unpublished), Vol. 2.
[27] W. P. Leung, M. Kulkarni, D. Krajnovich, and A. C. Tam, Appl Phys Lett. **58**, (1991).
[28] N. Leclerc, C. Pfleiderer, J. Wolfrum, K. Greulich, W. P. Leung, M. Kulkarni, and A. C. Tam, Appl. Phys Lett. **59**, 3369 (1991).
[29] M. Rotschild, D. J. Ehrlich, and D. C. Shaver, Appl Phys Lett. **55**, 1276 (1989).